ChemComm

Cite this: *Chem. Commun.*, 2012, **48**, 6669–6671

www.rsc.org/chemcomm

COMMUNICATION

Anthraquinone with tailored structure for a nonaqueous metal–organic redox flow battery†

Wei Wang,*[a] Wu Xu,*[a] Lelia Cosimbescu,[a] Daiwon Choi,[a] Liyu Li[b] and Zhenguo Yang[b]

Received 5th April 2012, Accepted 8th May 2012
DOI: 10.1039/c2cc32466k

A nonaqueous, hybrid metal–organic redox flow battery based on tailored anthraquinone structure is demonstrated to have an energy efficiency of ~82% and a specific discharge energy density similar to those of aqueous redox flow batteries, which is due to the significantly improved solubility of anthraquinone in supporting electrolytes.

Redox flow batteries (RFBs) have attracted considerable research interest primarily due to their ability to store large amounts of power and energy, up to multi-MW and multi-MWh, respectively.[1–3] RFB systems are considered one of the most promising technologies to be utilized not only for integrating renewable energy resources, but also to improve the efficiency of grid transmission and distribution.[4,5] With the energy supplied from externally stored electrolytes, the dissociation of energy capacity and power capability offers unique design latitude for RFBs to be sized for a wide spectrum of power and energy storage applications. Other advantages of RFBs include high safety, quick response, long service life, and deep discharge ability.

Limited by the water electrolysis potential window and the active materials' concentrations, the traditional aqueous RFBs are in general low energy density systems (<25 Wh L^{-1} in most true flow battery systems). Although significant progress has been made to improve the energy density of aqueous RFB systems,[1] it is often severely hindered by the poor solubility and stability of the active materials in the solutions. In this regard, a nonaqueous RFB system is attractive because it offers the expansion of the operating potential window, which has a direct impact on the system energy and power densities. Ruthenium-based active materials were investigated first by Matsuda *et al.* and then by Chakrabarti and co-workers as nonaqueous RFB electrolytes.[6,7] More recently, Thompson and co-workers reported RFBs based on redox couples of $M(acac)_3$ (M = V, Cr, or Mn; acac is acetylacetonate).[8–10] In addition, ionic liquids and organic redox agents have recently been reported as RFB supporting electrolytes and active materials, respectively.[11,12] In general, RFBs with operating voltages higher than 2.0 V have been demonstrated in various nonaqueous chemistries. However, the solubility of the active materials is dismal (<0.1 M of active materials in most cases) compared with aqueous systems where state-of-the-art all-vanadium RFBs demonstrated active-materials concentrations of >2.0 M as an example.[1] Reported cycling performance of the nonaqueous RFBs is often accompanied by poor voltage and energy efficiency, and significant degradation over cycling.[8–12]

Here we report a hybrid metal–organic redox flow battery (MORFB) based on a modified anthraquinone (AQ) molecule as the positive electrolyte and lithium metal as the negative electrode. Anthraquinone-based organic materials have been widely studied as lithium-ion battery (LIB) cathode materials.[13–17] The redox mechanism of AQ is well understood, as shown in Scheme 1, involving a two-electron disproportionation in two well defined steps during discharge processes: the formation of a radical anion in the first stage followed by dianion formation.[15] However, all the quinone-based compounds with short-chain substituents have very low solubility (less than 0.05 M) in most electrolytes of relatively high polarity. Modification of the AQ core is thus required to improve the solubility of AQ as the energy bearing redox active agent.

The molecule of choice for this study is 1,5-bis(2-(2-(2-methoxyethoxy)ethoxy)ethoxy)anthracene-9,10-dione (abbreviated as 15D3GAQ), shown in Scheme 2. Indeed the introduction of two triethylene glycol monomethyl ether groups into the AQ molecular structure had a large effect on the solubility, and the resulting molecule was soluble in most polar solvents and nonaqueous electrolytes. The compound was synthesized *via* nucleophilic aromatic substitution of 1,5-dichloroanthraquinone in the

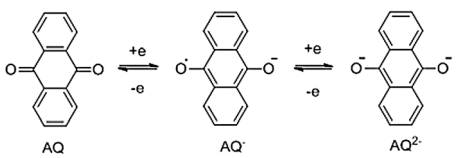

Scheme 1

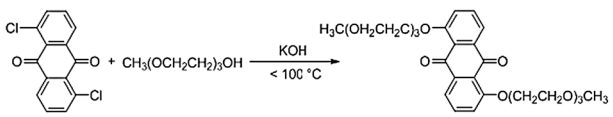

Scheme 2

[a] *Pacific Northwest National Laboratory, Richland, WA 99354, USA. E-mail: wei.wang@pnnl.gov, wu.xu@pnnl.gov; Fax: +1-509-375-2186, +1-509-375-3864; Tel: +1-509-372-4097, +1-509-375-6934*
[b] *UniEnergy Technologies, LLC, 4333 Harbour Pointe Blvd SW, Unit A, Mukilteo, WA 98275, USA*
† Electronic supplementary information (ESI) available: Full experimental details. See DOI: 10.1039/c2cc32466k

presence of triethylene glycol monomethyl ether as both reagent and solvent, and potassium hydroxide base to generate the nucleophile.[18] The mixture is typically stirred at a temperature slightly below 100 °C for 3 h to ensure completion of the reaction. After purification, the material was obtained as a pure yellow solid in a yield of over 80%. The experimental details and characterization are included in the ESI.†

The nonaqueous electrolyte preparation and redox flow cell assembly were all completed inside an MBraun glove box filled with purified argon of moisture and oxygen content less than 1 ppm. The RFB electrolyte was prepared by dissolving 15D3GAQ and $LiPF_6$ (battery grade, Novolyte, USA) in propylene carbonate (PC) (battery grade, Novolyte) at room temperature, with concentrations of 0.25 M 15D3GAQ and 1.0 M $LiPF_6$. The available redox reactions and their reversibility and the kinetics of 15D3GAQ were first investigated by cyclic voltammetry (CV) using a static cell. The cell was assembled with a 0.3 cm thick graphite felt disk (SGL Carbon Group, Germany) soaked with 0.2 mL of the above electrolyte as a working electrode and a piece of lithium disk as a counter electrode, with a polypropylene separator (Celgard 3401, USA) in between. The whole assembly was subsequently sealed in the cell compartment. A CHI660C electrochemical station (CH Instruments, USA) was used to identify redox couples and electrochemical reversibility in the voltage range between 1.3 V and 3.5 V at a scan rate of 0.1 mV s^{-1}.

Fig. 1 shows the CV curves of 15D3GAQ in 1.0 M $LiPF_6$/PC electrolyte during continuous scans, in which the current density was normalized to the geometrical area of the working electrode. During the first cathodic scan, two sharp peaks at 2.22 V (pc1) and 2.00 V (pc2) correspond to the reductions of the first and second –C═O groups to the ═C–O^- anions. The corresponding oxidative peaks are located at about 2.82 V (pa1) and 2.50 V (pa2). The peak separations for the two redox peaks are 0.60 V for pc1/pa1 and 0.50 V for pa2/pc2. Such a big difference between the redox peaks (~0.5 V) indicates the high polarization of this material during charge and discharge processes. During the following scans, the two reduction peaks are slightly shifted toward higher voltages and maintain at 2.27 V (pc1) and 2.03 V (pc2), respectively. The corresponding oxidative peaks are shifted toward slightly lower voltages and stay at about 2.79 V (pa2) and 2.47 V (pa1). Therefore, the peak separations for the two redox peaks are narrowed to 0.52 V for (pc1/pa1) and 0.44 V for (pa2/pc2), meaning a slight improvement in the polarization. There is a small oxidation peak at ~2.9 V and the intensity increases with scanning cycles, whose corresponding reduction peak however is not observed. This small irreversible oxidation peak is not related to Li insertion and de-insertion of 15D3GAQ, but probably corresponds to the reaction of the anthraquinone radical anion with the carbonate solvent.[17] Reported CV studies on the AQ-based cathode materials for LIBs typically show either one pair of redox peaks or two pairs but not well separated,[15,17] whereas the CV spectrum of 15D3GAQ shows two well defined redox peaks.

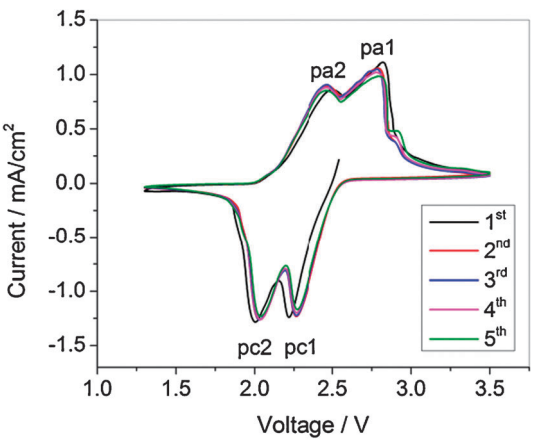

Fig. 1 CV curves of the 0.25 M 15D3GAQ in 1.0 M $LiPF_6$/PC electrolyte in the voltage range between 1.3 V and 3.5 V at 0.1 mV s^{-1}.

The electrochemical cycling performance of the 15D3GAQ static cell was evaluated using a constant-current method on a battery tester (Arbin Instruments, USA). The 15D3GAQ static cell was cycled in the voltage window between 1.8 V and 2.8 V at a constant current density of 0.1 mA cm^{-2}, and its electrochemical cycling performance is shown in Fig. 2. Corroborating with the CV scan result, two voltage plateaus are clearly observed in the typical cell voltage profile during charge and discharge processes (Fig. 2(a)). The voltage plateaus at ~2.4 V during discharge and ~2.45 V during charge correspond to the formation of radical anions, while the voltage plateaus at ~2.15 V during discharge and ~2.25 V during charge represent the dianion formation, as illustrated in Scheme 1. The voltage profiles demonstrated by the 15D3GAQ static cell exhibit voltage ranges similar to the previously reported AQ-based organic compounds used as LIB cathode materials.[15,17] However, while

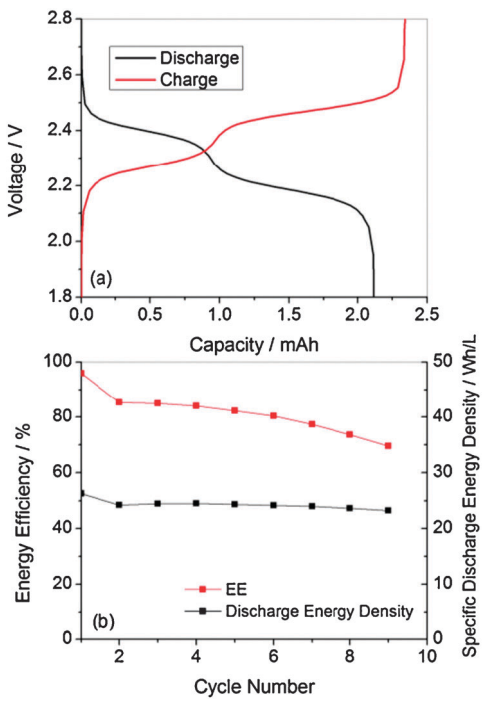

Fig. 2 The electrochemical performance of a MORFB with 0.25 M 15D3GAQ in 1.0 M $LiPF_6$/PC solution as a positive electrolyte and lithium metal as a negative electrode. (a) Cell voltage profile *versus* cell capacity during a typical charge–discharge process. (b) Cyclic energy efficiency and specific discharge energy density as a function of cycle number.

there is normally only one slope plateau observed with AQ-based LIB cathode materials in the literature, two distinct voltage plateaus were present in the flow battery static cell tests. Compared to the AQ-based cathodes for LIBs in previous literature reports, two well separated CV peaks and two distinct voltage plateaus were observed with the cell using 15D3GAQ as the positive electrolyte. The difference is attributed to the single molecule existence of 15D3GAQ in the electrolyte enabling more localized redox reaction, whereas the AQ-based LIB cathode is usually in the polymerized large molecular form and the delocalized electron density along the polymer chain.[15,17]

Fig. 2(b) shows the energy efficiency of the hybrid MORFB with 0.25 M 15D3GAQ in 1.0 M $LiPF_6$/PC solution as the positive electrolyte and lithium metal as the negative electrode in the static cell test, in which an overall energy efficiency of ~82% is achieved. The discharge energy density, representing the ultimate capability of the cell to deliver useful energy, is also plotted in Fig. 2(b). A specific volumetric energy density close to 25 Wh L^{-1} is obtained, for which the calculation was based on the positive electrolyte volume, and the result is comparable with the current aqueous RFB systems. The long term cycling data and rate capability test results are provided in Fig. S1, ESI.† The specific discharge capacity starts to drop after several cycles. Similar capacity fading has also been observed for AQ-polymer based cathodes in the LIBs, which is ascribed to the side reactions between the AQ structure and the carbonate solvents.[16,17] Rate capability of the cell was tested under different current densities as shown in Fig. S1 (ESI†). The cell was cycled at 0.1 mA cm^{-2} for the first cycle. The current was then ramped up to 10 mA cm^{-2} successively. Compared to the aqueous RFBs, which in general are capable of cycling at 50 mA cm^{-2}, the rate capability of the first reported MORFB is low, which is mainly due to the low diffusion rate of charge carrier Li^+ ions in the MORFB compared to that of the proton in the aqueous RFBs. An extensive study and optimization of the suitable supporting electrolytes with different combinations of salts and solvents are currently underway. The results will be published in due course.

In conclusion, we proposed, fabricated and investigated a hybrid MORFB in a static cell setup. Through the modification of the anthraquinone structure, 15D3GAQ was successfully synthesized. Due to its significantly improved solubility, 15D3GAQ can be employed as an energy-carrying active material for RFB application in the common $LiPF_6$ salt and carbonate supporting electrolyte. A static cell employing 0.25 M 15D3GAQ in 1.0 M $LiPF_6$/PC solution as a positive electrolyte and lithium metal as a negative electrode demonstrated an energy efficiency of ~82% and a specific discharge energy density of ~25 Wh L^{-1}. The cycling performance of the 15D3GAQ static cell calls for the extensive study and development of suitable supporting electrolytes. Based on the above discussed experimental design and results, we propose a new MORFB system utilizing redox reactions between metal and organic electro-active molecular redox reagents. The MORFBs employ redox active organic molecules at the positive half-cell and metal or metal ions at the negative half-cell or *vice versa*. The rationale for exploring the hybrid system is to capitalize on the difference in the redox potential, solubility, and stability of different material systems. The hybrid nature of the system makes it easy to identify two redox couples to construct an RFB with a designable voltage window. Moreover, RFBs using organic redox active agents are particularly attractive for stationary energy storage in offering a combination of environmental friendliness, flexibility in structure design, high safety, and natural abundance, which may become critical in future large-scale applications.

The authors would like to acknowledge financial support from the U.S. Department of Energy's (DOE's) Office of Electricity Delivery & Energy Reliability (OE) (under Contract No. 57558). We are also grateful for useful discussions with Dr Imre Gyuk of the DOE-OE Grid Storage Program. PNNL is a multi-program national laboratory operated by Battelle for DOE under Contract DE-AC05-76RL01830.

Notes and references

1 L. Li, S. Kim, W. Wang, M. Vijayakumar, Z. Nie, B. Chen, J. Zhang, G. Xia, J. Hu, G. Graff, J. Liu and Z. Yang, *Adv. Energy Mater.*, 2011, **1**, 394–400.
2 W. Wang, S. Kim, B. Chen, Z. Nie, J. Zhang, G.-G. Xia, L. Li and Z. Yang, *Energy Environ. Sci.*, 2011, **4**, 4068–4073.
3 W. Wang, Z. Nie, B. Chen, F. Chen, Q. Luo, X. Wei, G.-G. Xia, M. Skyllas-Kazacos, L. Li and Z. Yang, *Adv. Energy Mater.*, 2012, **2**, 487–493.
4 B. Dunn, H. Kamath and J.-M. Tarascon, *Science*, 2011, **334**, 928–935.
5 Z. Yang, J. Zhang, M. C. W. Kintner-Meyer, X. Lu, D. Choi, J. P. Lemmon and J. Liu, *Chem. Rev.*, 2011, **111**, 3577–3613.
6 Y. Matsuda, K. Tanaka, M. Okada, Y. Takasu, M. Morita and T. Matsumura-Inoue, *J. Appl. Electrochem.*, 1988, **18**, 909–914.
7 M. H. Chakrabarti, R. A. W. Dryfe and E. P. L. Roberts, *Electrochim. Acta*, 2007, **52**, 2189–2195.
8 Q. Liu, A. E. S. Sleightholme, A. A. Shinkle, Y. Li and L. T. Thompson, *Electrochem. Commun.*, 2009, **11**, 2312–2315.
9 Q. Liu, A. A. Shinkle, Y. Li, C. W. Monroe, L. T. Thompson and A. E. S. Sleightholme, *Electrochem. Commun.*, 2010, **12**, 1634–1637.
10 A. E. S. Sleightholme, A. A. Shinkle, Q. Liu, Y. Li, C. W. Monroe and L. T. Thompson, *J. Power Sources*, 2011, **196**, 5742–5745.
11 Z. Li, S. Li, S. Liu, K. Huang, D. Fang, F. Wang and S. Peng, *Electrochem. Solid-State Lett.*, 2011, **14**, A171–A173.
12 D. Zhang, Q. Liu, X. Shi and Y. Li, *J. Power Sources*, 2012, **203**, 201–205.
13 H. Alt, H. Binder, A. Köhling and G. Sandstede, *Electrochim. Acta*, 1972, **17**, 873–887.
14 T. Le Gall, K. H. Reiman, M. C. Grossel and J. R. Owen, *J. Power Sources*, 2003, **119–121**, 316–320.
15 Z. Song, H. Zhan and Y. Zhou, *Chem. Commun.*, 2009, 448–450.
16 Z. Lei, W. Wei-kun, W. An-bang, Y. Zhong-bao, C. Shi and Y. Yu-sheng, *J. Electrochem. Soc.*, 2011, **158**, A991–A996.
17 W. Xu, A. Read, P. K. Koech, D. H. Hu, C. M. Wang, J. Xiao, A. B. Padmaperuma, G. L. Graff, J. Liu and J. G. Zhang, *J. Mater. Chem.*, 2012, **22**, 4032–4039.
18 M.-Y. You, L. Wang, G.-Y. Peng, J.-F. Wang and Y.-Q. Liu, *Fine Chem.*, 2010, **1**, 101–104 (in Chinese).